research papers

Morphology of polysorbate 80 (Tween 80) micelles in aqueous 1,4-dioxane solutions

Hideki Aizawa

Department of Pharmaceutical Physical Chemistry, Faculty of Pharmaceutical Sciences, Setsunan University, 573-0101, Osaka, Japan. Correspondence e-mail: aizawa@pharm.setsunan.ac.jp

The structures of micelles of the surfactant polysorbate 80 (Tween 80) in 0–50% aqueous 1,4-dioxane solutions (pH 7.2, ionic strength 2.44 mM) were investigated by means of small-angle X-ray scattering. At 1,4-dioxane concentrations of 0–20%, core–shell cylindrical micelles formed because the crown-shaped polysorbate 80 molecules aggregated into a cylindrical layer of four chains entangled with one another through intra- and intermolecular interactions. At 30–40% 1,4-dioxane, core–shell discus micelles formed, and at 50% 1,4-dioxane, core–shell elliptic discus micelles formed by the same mechanism. By changing the 1,4-dioxane solvent concentration and increasing the solvent hydrophobicity, the micelles first change from core–shell cylindrical to core–shell discus and then from core–shell discus to core–shell elliptic discus micelles.

1. Introduction

Surfactants are amphipathic molecules (they contain both a hydrophobic and a hydrophilic group) and form micelles (hydrophobic core/hydrophilic shell micelles) in aqueous solutions. Colloidal researchers are interested in investigating how the change from aqueous solutions to organic solvents affects micellar shape and size. However, many mixtures of organic solvents and water promptly separate into phases since the solvents are not miscible with water. They never actually form solutions and thus micellar behaviour in such solutions is not of interest in colloidal and surface research. However, polar organic solvents are soluble in water, and thus micellar behaviour in aqueous solutions of these solvents is of scientific interest. Polar organic solvents (such as ethylene glycol, glycerol, formamide and hydrazine) have been found to promote the micellization of surfactants (Gopal & Singh, 1973; Ramadan et al., 1983, 1985; Almgren et al., 1985; Rico & Lattes, 1986; Auvray et al., 1987; Binana-Limbele & Zana, 1989; Fletcher & Gilbert, 1989; Lattes & Rico, 1989; Martino & Kaler, 1990; Takisawa et al., 1993; Penford et al., 1997; Carnero Ruiz et al., 2003; Rodriguez et al., 2003; D'Errico et al., 2005; Glenn et al., 2005; Seguin et al., 2006, 2007). 1,4-Dioxane is a polar organic solvent and is normally used as a solvent of wax, oils and spirit-sol dyes. Aqueous solutions of 1,4-dioxane are normally used as the reference solutions for gauging the apparent water activity and micropolarity of aqueous environments in surfactant self-assembly systems by means of the fluorescent probe method (Galvin et al., 1987; Hanke et al., 1987; Grieser & Drummond, 1988; Drummond et al., 1991; Chakrabarty et al., 2008). Thus, it is important to understand the changes in micellar shape and size that occur with changes in the 1,4-dioxane solvent concentration in aqueous solutions. Polysorbate 80 (Tween 80; the typical polysorbate 80 molecular structure is illustrated in Fig. 1) is a hydrophilic non-ionic surfactant and is frequently used as an emulsifier and dispersing agent for medicinal products designed for internal use (O'Neil et al., 2006).

Thus, information about how polysorbate 80 micelles form and how changing the solvent from 100% water to mixtures of water and 1,4-dioxane affects the shape and size of polysorbate 80 micelles can be expected to be of use not only for improving the understanding of the underlying basic principles of the phenomenon, but also for practical application to wax, toiletries and other industrial products. Small-angle X-ray scattering (SAXS) can be used to determine the three-dimensional structure and size distribution of micelles in solution. In this study, we used SAXS to investigate the structure of polysorbate 80 micelles in aqueous 1,4-dioxane at pH 7.2 and ionic strength 2.44 mM.

2. Materials and method

2.1. Materials

Polysorbate 80 (Tween 80) and 1,4-dioxane were obtained from Nacalai Tesque (Kyoto, Japan), and disodium hydrogen phosphate ($Na_2HPO_4 \cdot 12H_2O$) and sodium dihydrogen phosphate ($NaH_2PO_4 \cdot 2H_2O$) were obtained from Wako Pure Chemical Industries (Osaka, Japan).

2.2. Sample preparation

A mixture of 7.2 mmol $Na_2HPO_4 \cdot 12H_2O$ and 2.8 mmol $NaH_2PO_4 \cdot 2H_2O$ was dissolved in 1 l of water to give a 10 mM stock solution of sodium phosphate buffer (pH 7.2, ionic strength 24.4 mM). Polysorbate 80 was dissolved in the stock

sodium phosphate buffer to give a 500 g l^{-1} stock solution. The stock sodium phosphate buffer, stock polysorbate 80 solution, 1,4-dioxane and water were mixed to give sample solutions that contained 0–50% 1,4-dioxane, 50 g l^{-1} polysorbate 80 and 1 mM sodium phosphate buffer (pH 7.2, ionic strength 2.44 mM). The stock sodium phosphate buffer, 1,4-dioxane and water were mixed to give reference solutions that contained 0–50% 1,4-dioxane and 1 mM sodium phosphate buffer.

2.3. SAXS measurements

The small-angle X-ray scattering equipment for solutions (SAXES) optics and detector system installed at the Energy Accelerator Research Organization in Tsukuba, Japan, was used for the SAXS experiments, which were conducted at 298 K. An X-ray wavelength of 0.149 nm was used. A one-dimensional position-sensitive proportional counter with an effective length of 200 nm (Rigaku Denki, Tokyo, Japan) was used to register the X-ray scattering intensity at 512 different

$CH_2(OC_2H_4)_5OOCC_{17}H_{33}$
42.3 Å

$(OC_2H_4)_5OH$
17.6 Å

$(OC_2H_4)_5OH$
17.6 Å

$(OC_2H_4)_5OH$
17.6 Å

● Carbon ◉ Oxygen ○ Hydrogen

Figure 1
Typical polysorbate 80 molecular structure.

angles. The specifications of this equipment are detailed by Kajiwara & Hiragi (1996) and Ueki (1991).

SAXS intensities were measured for 600 s for each surfactant solution and for a reference solution, and intensities were then calibrated and transformed into scattering cross sections [SCS(q), where q is the scattering vector] based on the scattering cross section of water (Dreiss *et al.*, 2006). To calculate the SCS(q) of solute, the scattering cross section of the reference solution was subtracted from the scattering cross section of the surfactant solution. Units of cm^{-1} are normally used for SCS(q) (Lindner & Zemb, 2002), but because the q vector is in Å^{-1} and particle size is frequently given in Å, we have used Å^{-1} for SCS(q) to avoid possible mistakes in unit conversions.

2.4. Analysis of the SAXS data

We attempted to fit the SAXS data to each of the following models: the monodisperse core–shell sphere, the polydisperse sphere, the core–shell tri-axial ellipsoid, the core–shell cylinder by means of random phase approximation (RPA), the core–shell cylinder by means of polymer reference interaction site model (PRISM), the core–shell elliptic cylinder by means of RPA, the core–shell elliptic cylinder by means of PRISM, and the star polymer (Pedersen, 1997; Lindner & Zemb, 2002).

Least-squares fit calculations showed that the core–shell cylinder model of dilute particle solutions provided the best fit for the SAXS data at 1,4-dioxane concentrations of 0–40%, and the core–shell elliptic cylinder model of dilute particle solutions provided the best fit for the SAXS data at 50% 1,4-dioxane. The mathematical descriptions of the core–shell cylinder and the core–shell elliptic cylinder models of dilute particle solutions are given below.

SCS(q), which does not take into account the structure factor (in dilute particle solutions), is given by

$$\text{SCS}(q) = nV^2\Delta\beta^2 F(q)^2, \qquad (1)$$

where q is the scattering vector [$q = (4\pi/\lambda)\sin\theta$ (where λ is the wavelength of the X-rays and 2θ is the scattering angle)]; n, $\Delta\beta$ and V are the number density of particles, the difference in scattering length density between the particles and the solvent or matrix, and the volume of particles, respectively; and $F(q)$ is the form factor.

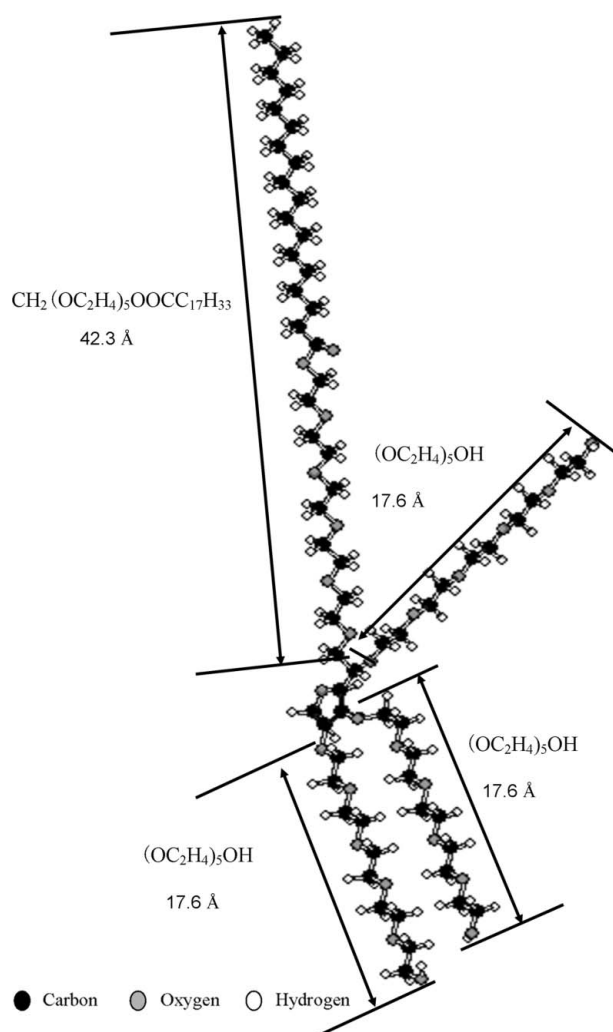For the core–shell cylinder (Feigin & Svergun, 1987), V and $\Delta\beta^2 F(q)^2$ are given by

$$V = \pi(R+d)^2 H \qquad (2)$$

and

$$\Delta\beta^2 F(q)^2 = \int_0^1 \left\{[CF_1(q) + CF_2(q)]/CF_3(q)\right\}^2 dx, \qquad (3)$$

where

$$CF_1(q) = \left\{4R(\beta_{core} - \beta_{shell})J_1[qR(1-x^2)^{1/2}] \right.$$
$$\left. \times \sin(qHx/2)\right\}/[q^2x(1-x^2)^{1/2}], \qquad (4)$$

Table 1
Density and scattering length density of polysorbate 80.

Density (g cm^{-3})	Scattering length density (μ Å^{-2})
1.073	10.12

Table 2
Densities and scattering length densities of the reference solvent.

	1,4-Dioxane concentration (%)					
	0	10	20	30	40	50
Density (g cm^{-3})	0.996	1.005	1.014	1.022	1.028	1.033
Scattering length density (μ Å^{-2})	9.216	9.527	9.826	10.14	10.44	10.69

$$CF_2(q) = \left\{4(R + d)(\beta_{shell} - \beta_{solvent})J_1[q(R + d)(1 - x^2)^{1/2}] \times \sin(qHx/2)\right\}/[q^2x(1 - x^2)^{1/2}], \quad (5)$$

$$CF_3(q) = R^2 H(\beta_{core} - \beta_{shell}) + (R + d)^2 H(\beta_{shell} - \beta_{solvent}), \quad (6)$$

where R and β_{core} are the radius of the circular base of the core cylinder and the scattering length density of the core, respectively; d and β_{shell} are the length and the scattering length density of the shell, respectively; H is the height of the core–shell cylinder; and x is the distance on the x axis. J_1 is the first-order Bessel function and $\beta_{solvent}$ is the scattering length density of the solvent.

Six parameters (n, R, d, H, β_{core} and β_{shell}) for equations (1)–(6) were determined by a least-squares fit of the SAXS data to the model. Rough values of β_{core} and β_{shell} were estimated and the exact value of $\beta_{solvent}$ was determined from the density and the number of electrons of polysorbate 80 and the mixed solvents (Lindner & Zemb, 2002). $\beta_{core} = (\rho_{core} \, \mathrm{Ne}_{core} \, \mathrm{Th} \, N_A)/M_{core}$, $\beta_{shell} = (\rho_{shell} \, \mathrm{Ne}_{shell} \, \mathrm{Th} \, N_A)/M_{shell}$ and $\beta_{solvent} = (\rho_{solvent} \, \mathrm{Ne}_{solvent} \, \mathrm{Th} \, N_A)/M_{solvent}$, where ρ is the density (of the core, shell or solvent), Ne the electron number of the molecule (of the core, shell or solvent), Th the Thomson radius, N_A the Avogadro number and M the molecular weight (of the core, shell or solvent).

For the core–shell elliptic cylinder (Feigin & Svergun, 1987), V and $\Delta\beta^2 F(q)^2$ are given by

$$V = \pi\varepsilon(a + d)^2 H \quad (7)$$

and

$$\Delta\beta^2 F(q)^2 = \int_0^1 \int_0^\pi \left\{[CF_4(q) + CF_5(q)]/CF_6(q)\right\}^2 \, dy \, dx, \quad (8)$$

where

$$CF_4(q) = 4\pi a(\beta_{core} - \beta_{shell})J_1\left\{qa[0.5(1 - \varepsilon^2) + 0.5(1 - \varepsilon^2)\cos y]^{1/2}\right\}\sin(qHx/2), \quad (9)$$

$$CF_5(q) = 4\pi(a + d)(\beta_{shell} - \beta_{solvent})J_1\left\{q(a + d)[0.5(1 - \varepsilon^2) + 0.5(1 - \varepsilon^2)\cos y]^{1/2}\right\}\sin(qHx/2), \quad (10)$$

$$CF_6(q) = [a^2(\beta_{core} - \beta_{shell}) + (a + d)^2(\beta_{shell} - \beta_{solvent})] \times \pi^{1/2}q^2Hx[0.5(1 - \varepsilon^2) + 0.5(1 - \varepsilon^2)\cos y]^{1/2}, \quad (11)$$

where a, ε and β_{core} are the length along the x axis, the ratio of the length along the z axis to the length along the x axis of the elliptic base of the core elliptic cylinder, and the scattering length density of the core, respectively; d and β_{shell} are the length and the scattering length density of the shell, respectively; H is the height of the core–shell elliptic cylinder; and x

and y are the distances on the x and y axes. J_1 is the first-order Bessel function and $\beta_{solvent}$ is the scattering length density of the solvent.

Seven parameters (n, a, ε, d, H, β_{core} and β_{shell}) for equations (7)–(11) were determined by means of a least-squares fit of the SAXS data to the model. Rough values of β_{core} and β_{shell} were estimated and the exact value of $\beta_{solvent}$ was determined from the density and the number of electrons of the polysorbate 80 molecule and the mixed solvents (Lindner & Zemb, 2002).

The scattering length densities of the polysorbate 80 molecule and the reference solvent can be estimated from the components, the density and the number of electrons. $\beta_{core} = (\rho_{core} \, \mathrm{Ne}_{core} \, \mathrm{Th} \, N_A)/M_{core}$, $\beta_{shell} = (\rho_{shell} \, \mathrm{Ne}_{shell} \, \mathrm{Th} \, N_A)/M_{shell}$ and $\beta_{solvent} = (\rho_{solvent} \, \mathrm{Ne}_{solvent} \, \mathrm{Th} \, N_A)/M_{solvent}$, where ρ is the density (of the core, shell or solvent), Ne the electron number of the molecule (of the core, shell or solvent), N_A the Avogadro number, Th the Thomson radius and M the molecular weight (of the core, shell or solvent). The values are listed in Tables 1 and 2, respectively (Lindner & Zemb, 2002). The densities of polysorbate 80 and the reference solutions were determined with a pycnometer.

Algorithms for the least-squares fit calculations for the models and the SAXS data were based on a simplex method (polytope method) and many algorithms for numerical calculations (integral calculation, Bessel function etc.) using the Visual Basic 6.0 program package (Nash, 1987; Gill et al., 1981; Okumura, 1991; Tankei et al., 1993).

3. Results and discussion

It was concluded that the shape of the polysorbate 80 micelle is a core–shell spherical structure based on consideration of the distinguishing features of the pair-distance distribution function (PDDF) curves transformed from the SAXS intensity, q vectors and other parameters. The PDDF curves of polysorbate 80 indicated a local maximum and minimum on the low-r side and a short tail on the high-r side of the PDDF curves, which are regarded as typical features of a core–shell spherical structure. Thus, the shape of the polysorbate 80 micelle was considered to be a core–shell spherical particle (Varade et al., 2007).

However, there is another method to determine micellar shape in solution. The geometric model of a core–shell sphere directly fits the SAXS data. We attempted to fit the SAXS data to each of the core–shell spheres that do not take account of

Table 3
Shape parameters at various 1,4-dioxane concentrations.

The core–shell cylinder model $[S(q) = 1]$.

Concentration (%)	n (aÅ^{-3})	R (Å)	d (Å)	H (Å)	Volume (kÅ^3)	β_{core} (μ Å^{-2})	β_{shell} (μ Å^{-2})
0	352	10	32	57	316	7.656	9.497
10	287	10	31	53	280	7.967	9.808
20	175	11	29	50	251	8.266	10.11
30	338	14	30	12	43	8.306	10.14
40	294	16	25	9	49	8.306	11.29

The core–shell elliptic cylinder model $[S(q) = 1]$.

| Concentration (%)	n (aÅ^{-3})	a (Å)	d (Å)	ε	H (Å)	Volume (kÅ^3)	β_{core} (μ Å^{-2})	β_{shell} (μ Å^{-2})
50	45	14	32	0.006	10	0.4	8.306	11.19

the structure factor $[S(q) = 1]$ and the core–shell spheres that take account of the structure factor $[S(q) \neq 1]$. The SAXS data did not fit either of the core–shell sphere models (data not shown). The shape of the polysorbate 80 micelle was not a core–shell sphere.

We attempted to fit the SAXS data to each of the core–shell cylinder and core–shell elliptic cylinder models of dilute particle solutions. Scattering data obtained at 1,4-dioxane concentrations between 0 and 50% are shown in Fig. 2, along with curves fitted with the core–shell cylinder and the core–shell elliptic cylinder models. The 1,4-dioxane concentrations and shape parameters calculated from the core–shell cylinder and the core–shell elliptic cylinder models of dilute particle solutions are listed in Table 3. The core–shell cylinder model of dilute particle solutions provided the best fit for the SAXS data at 0–40% 1,4-dioxane, and the core–shell elliptic cylinder model in dilute particle solutions provided the best fit for the

SAXS data at 50% 1,4-dioxane. Fig. 3 shows schematic diagrams of polysorbate 80 micelles in 0–50% 1,4-dioxane solutions. The SAXS data indicated that, at 0–20% 1,4-dioxane, the polysorbate 80 formed core–shell cylindrical micelles. Because $(R + d) > H$ (see Table 3), we concluded that, at 30–40% 1,4-dioxane, the polysorbate 80 formed core–shell discus micelles rather than core–shell cylindrical micelles. Because $(a + d) > H$ (see Table 3), we concluded that, at 50% 1,4-dioxane, the polysorbate 80 formed core–shell elliptic discus micelles rather than elliptic core–shell cylindrical micelles. Thus, changing the 1,4-dioxane solvent concentration and increasing the solvent hydrophobicity changed the micelles from core–shell cylindrical micelles to core–shell discus micelles between 20 and 30% 1,4-dioxane, and from core–shell discus micelles to core–shell elliptic discus micelles between 40 and 50% 1,4-dioxane; the solvent change also resulted in a decrease in the size of the micelles.
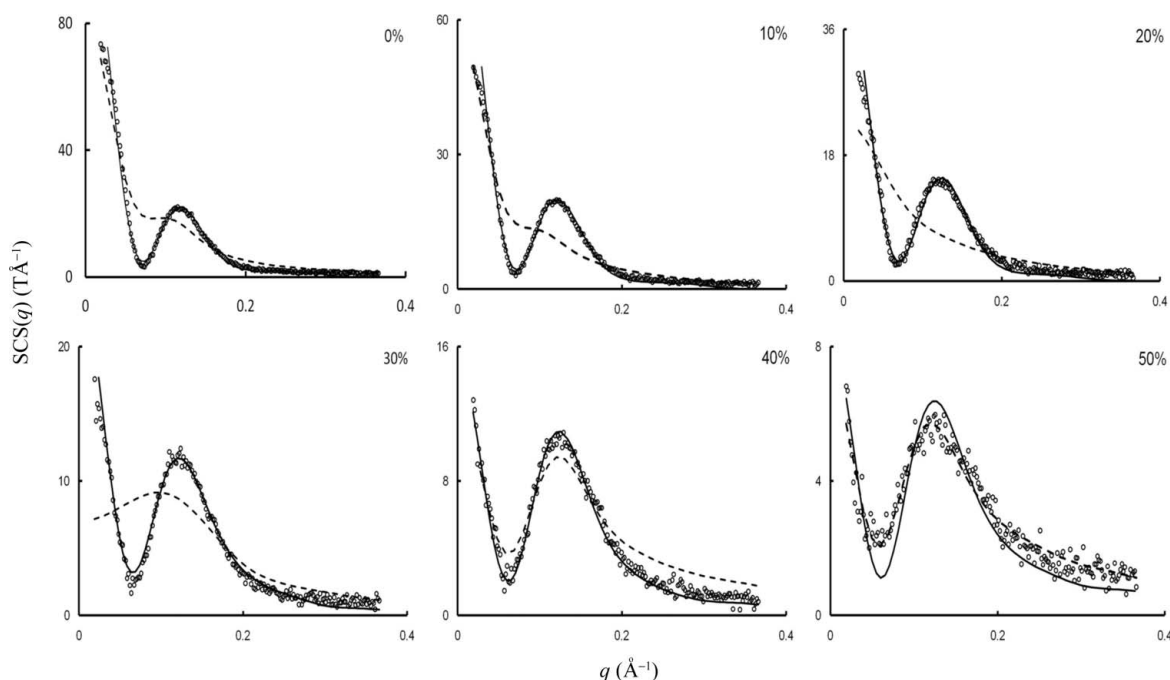
Figure 2
Scattering data (circles) obtained at 1,4-dioxane concentrations between 0 and 50%, along with curves fitted with a core–shell cylinder model, $S(q) = 1$ (line), and a core–shell elliptic cylinder model, $S(q) = 1$ (dashed line).
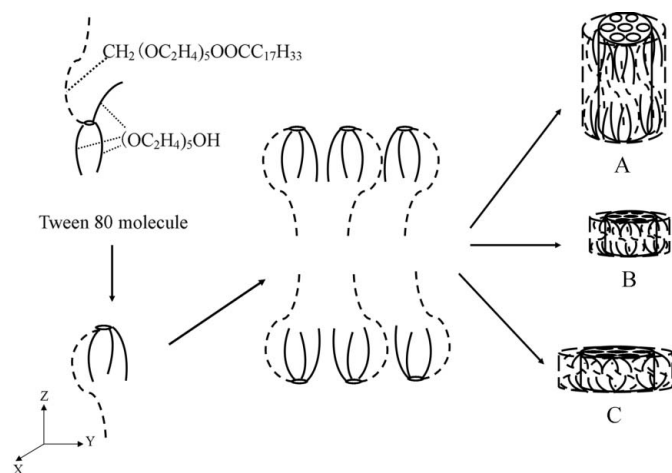
Figure 3
Formation of core–shell cylindrical micelles, core–shell discus micelles and core–shell elliptic discus micelles from polysorbate 80 molecules. A, at 0–20% 1,4-dioxane concentrations core–shell cylindrical micelle; B, at 30–40% 1,4-dioxane concentrations core–shell discus micelle; C, at 50% 1,4-dioxane concentrations core–shell elliptic discus micelle.

Fig. 3 illustrates the formation of core–shell cylindrical micelles from polysorbate 80 molecules. At 0–20% 1,4-dioxane, the polysorbate 80 molecules adopted crown-like shapes and aggregated into a 'cylindrical' layer of four long chains entangled with one another through intra- and inter-molecular interactions. At 30–40% and 50% 1,4-dioxane, core–shell discus micelles and core–shell elliptic discus micelles, respectively, were formed by a similar mechanism.

4. Conclusions

We used SAXS to investigate how changing the solvent from 100% water to a mixture of water and 1,4-dioxane affected the shape and size of polysorbate 80 micelles. As the concentration of 1,4-dioxane was increased, the micelles changed from core–shell cylindrical micelles to core–shell discus micelles to core–shell elliptic discus micelles, and there was a concomitant decrease in the size of the micelles. It is significant that a change in the hydrophobicity of 1,4-dioxane affected both the shape and the size of polysorbate 80 micelles. There is a strong possibility that a change in the hydrophobicity of other polar organic solvents will affect the shape and size of polysorbate 80 micelles.

References

Almgren, M., Swarup, S. & Lofroth, J. E. (1985). *J. Phys. Chem.* **89**, 4621–4626.
Auvray, X., Petipas, C., Anthore, R., Rico, I., Lattes, A., Samii, A. A. Z. & De Savignac, A. (1987). *Colloid Polym. Sci.* **265**, 925–932.
Binana-Limbele, W. & Zana, R. (1989). *Colloid Polym. Sci.* **267**, 440–447.
Carnero Ruiz, C., Molina-Bolívar, J. A., Aguiar, J., MacIsaac, G., Moroze, S. & Palepu, R. (2003). *Colloid Polym. Sci.* **281**, 531–541.
Chakrabarty, A., Das, P., Mallick, A. & Chattopadhyay, N. (2008). *J. Phys. Chem. B*, **112**, 3684–3692.
D'Errico, G., Ciccarelli, D. & Ortona, O. (2005). *J. Colloid Interface Sci.* **286**, 747–754.
Dreiss, C. A., Jack, K. S. & Parker, A. P. (2006). *J. Appl. Cryst.* **39**, 32–38.
Drummond, C. J., Grieser, F. & Albers, S. (1991). *Colloids Surf.* **54**, 197–208.
Feigin, L. A. & Svergun, D. I. (1987). *Structure Analysis by Small-angle X-ray and Neutron Scattering*, edited by G. W. Taylor, p. 92. New York: Plenum Press.
Fletcher, P. D. I. & Gilbert, P. J. (1989). *J. Chem. Soc. Faraday Trans. 1*, **185**, 147–156.
Galvin, K., McDonald, J. A., Robinson, B. H. & Knoche, W. (1987). *Colloids Surf.* **25**, 195–204.
Gill, P. E., Murray, W. & Wright, M. H. (1981). *Practical Optimization*. London: Academic Press.
Glenn, K. M., Moroze, S., Bhattacharya, S. C. & Palepu, R. (2005). *J. Dispersion Sci. Technol.* **26**, 79–89.
Gopal, R. & Singh, J. R. (1973). *J. Phys. Chem.* **77**, 554–556.
Grieser, F. & Drummond, C. J. (1988). *J. Phys. Chem.* **92**, 5580–5593.
Hanke, V. R., Knoche, W. & Dutkiewicz, E. (1987). *J. Chem. Soc. Faraday Trans. 1*, **83**, 2847–2856.
Kajiwara, K. & Hiragi, Y. (1996). *Applications of Synchrotron Radiation to Materials Analysis*, edited by H. Saisho & Y. Gohshi, pp. 353–404. Amsterdam: Elsevier Science BV.
Lattes, A. & Rico, I. (1989). *Colloid Surf.* **35**, 221–235.
Lindner, P. & Zemb, T. (2002). *Neutron, X-rays and Light: Scattering Methods Applied to Soft Condensed Matter*. Amsterdam: Elsevier Science.
Martino, A. & Kaler, E. W. (1990). *J. Phys. Chem.* **94**, 1627–1631.
Nash, J. C. (1987). *Nonlinear Parameter Estimation: An Integrated System in Basic*. New York: Marcel Dekker.
Okumura, H. (1991). *The Recent Computer Algorithms in C*. Software Technology Series, p. 260. Tokyo: Gijyutsu–hyouronsha. (In Japanese.)
O'Neil, M. J., Heckelman, P. E., Koch, C. B., Roman, K. J., Kenny, C. M. & D'Arecca, M. R. (2006). *The Merck Index*, p. 7582. New Jersey: Merck and Co. Inc.
Pedersen, J. S. (1997). *Adv. Colloid Interface Sci.* **70**, 171–210.
Penford, J., Staples, E., Tucker, I. & Cummins, P. (1997). *J. Colloid Interface Sci.* **185**, 424–431.
Ramadan, M. S., Evans, D. F. & Lumry, R. (1983). *J. Phys. Chem.* **87**, 4538–4543.
Ramadan, M. S., Evans, D. F., Lumry, R. & Philson, S. (1985). *J. Phys. Chem.* **89**, 3405–3408.
Rico, I. & Lattes, A. (1986). *J. Phys. Chem.* **90**, 5870–5872.
Rodriguez, A., Graciani, M. M., Muñoz, M. & Moyá, M. L. (2003). *Langmuir*, **19**, 7206–7213.
Seguin, C., Eastoe, J., Clapperton, R., Heenan, R. K. & Grillo, I. (2006). *Colloids Surf. A*, **282**, 134–142.
Seguin, C., Eastoe, J., Heenan, R. K. & Grillo, I. (2007). *J. Colloid Interface Sci.* **315**, 714–720.
Takisawa, N., Thomason, M., Bloor, D. M. & Wyn-Jones, E. (1993). *J. Colloid Interface Sci.* **157**, 77–81.
Tankei, K., Okumura, H., Sato, T., Kobayashi, M., Press, W. H., Flannery, B. P., Teukolsky, S. A. & Vetterling, W. T. (1993). *Numerical Recipes in C*. Tokyo: Gijyutsu–hyouronsha. (In Japanese, translated from English.)
Ueki, T. (1991). *Nucl. Instrum. Methods Phys. Res. Sect. A*, **303**, 464–475.
Varade, D., Ushiyama, K., Shrestha, L. K. & Aramaki, K. (2007). *J. Colloid Interface Sci.* **312**, 489–497.